Available online at www.sciencedirect.com
SCIENCE DIRECT®
Journal of the European Ceramic Society 25 (2005) 19–28
www.elsevier.com/locate/jeurceramsoc

The influence of Y_2O_3-containing sintering additives on the oxidation of Si_3N_4-based ceramics and the interfacial interactions with liquid Al-alloys

M. Oliveira, S. Agathopoulos, J. M. F. Ferreira*

Department of Ceramics and Glass Engineering, CICECO, University of Aveiro, 3810-193 Aveiro, Portugal

Received 22 January 2004; received in revised form 10 March 2004; accepted 21 March 2004
Available online 18 May 2004

Abstract

Sintering additives containing Y_2O_3 influence the microstructure and the crystalline-state of Si_3N_4-ceramics produced via pressureless sintering, and determine their response towards oxidation. Y_2SiO_5 and $Y_2Si_2O_7$ were formed after sintering and oxidation, respectively. The superficial layers formed after oxidation are thinner and formed faster on the surface of the compositions $90Si_3N_4$–$5Y_2O_3$–$5Al_2O_3$ and $90Si_3N_4$–$5Y_2O_3$–5AlN than on $90Si_3N_4$–$5Y_2O_3$–$2.5Al_2O_3$–2.5AlN (in wt.%). The $90Si_3N_4$–$5Y_2O_3$–$5Al_2O_3$/liquid Al interface features strong interfacial adhesion while mild diffusion should govern the interfacial interactions. Compounds, whose formation results from the yttria-containing sintering aids, such as yttrium aluminates, should act as diffusion barriers at the ceramic/liquid metal interface. The experimental results indicate attractive features for applications in both Al-foundry industry and production of Si_3N_4–Al composites.

Keywords: Interfaces; Microstructure; Si_3N_4; Oxidation; Aluminium alloys

1. Introduction

The study of Si_3N_4/liquid Al interfaces attracts special technological interest in both ceramic joining field and aluminium-foundry industry. The research group of Suganuma and coworkers[1–6] investigated the production of joints of Si_3N_4 ceramics using Al-braze. Morita et al.[1] measured the non-wetted areas in the joints and concluded that preheating of Si_3N_4 remarkably improves wettability of Si_3N_4 by liquid Al and accordingly increase the mechanical strength of the joints. Ning et al.[2] compared the microstructure and the mechanical strength of similar (i.e., with Al) joints using pure Si_3N_4-ceramics and Si_3N_4 with Y_2O_3 and Al_2O_3 as sintering additives. According to the chemical analysis, the reaction-zone formed at the ceramic/metal interface comprised all the involved elements (i.e., Si, Al, N, Y and O).

Schwabe et al. have studied the interfacial interactions of eight different types of Si_3N_4 ceramics with Al-melts.[7] Their results showed that enhanced open porosity of ceramics favours the reaction with Al, which occurs in relatively short times. In the case of dense Si_3N_4, a dense and thin AlN layer formed at ceramic/metal interface seemingly functioned as a diffusion barrier. In that study, however, there is no clear evidence of the influence of sintering additives.

Johnson and Little investigated the performance of tubes made of Si_3N_4–SiC composites (with no sintering aids) which can provide indirect heating in non-ferrous foundry.[8] The samples were oxidized for several times and then immersed into liquid Al. The experimental results showed that prolonged pre-oxidation of ceramics favours the reaction with liquid Al and therefore reduce the mechanical properties of ceramics after their contact with molten Al. Non-preoxidized ceramics showed higher stability towards liquid Al.

The development of ceramic devices which can be reliably used in Al-foundry industry motivated the present study. In the frame of this particular application, ceramic/metal reactions are not generally desired, since they reduce the lifetime of ceramic components while the reaction products can contaminate the Al-melt. Therefore, the use of ceramics based on Si_3N_4 can be proposed for these applications

* Corresponding author. Tel.: +351-234-370242; fax: +351-234-425300.
E-mail address: jmf@cv.ua.pt (J.M.F. Ferreira).

0955-2219/$ – see front matter © 2004 Elsevier Ltd. All rights reserved.
doi:10.1016/j.jeurceramsoc.2004.03.021

since they can potentially combine high chemical inertness against liquid aluminium and very good mechanical properties. The aforementioned earlier studies[1–8] indicated that the performance of Si_3N_4 devices in Al-industry should depend on porosity and pre-oxidation. Porosity deals with infiltration process and pre-oxidation with the alterations of chemistry, crystallinity and topography of the surface, which can change the wettability and the interfacial interactions.

The kinetics of the oxidation of Si_3N_4-based ceramics generally follows a parabolic law:[9]

$$W^2 = Kt + B \quad (1)$$

where W is the weight gained due to oxidation, t is the exposure time to the oxidation atmosphere, and K and B are constants dependent on material and temperature. Several chemical reactions have been proposed to describe the oxidation of Si_3N_4:[10]

$$2Si_3N_4\,(s) + 1.5O_2\,(g) \leftrightarrows 3Si_2N_2O\,(s) + N_2\,(g) \quad (2)$$

$$3Si_2N_2O\,(s) + 4.5O_2\,(g) \leftrightarrows 6SiO_2\,(s) + 3N_2\,(g) \quad (3)$$

$$Si_3N_4\,(s) + 3O_2\,(g) \leftrightarrows 3SiO_2\,(s) + 2N_2\,(s) \quad (4)$$

$$Si_3N_4\,(s) + 3SiO_2\,(g) \leftrightarrows 6SiO\,(g) + 2N_2\,(g) \quad (5)$$

$$2Si_3N_4\,(s) + 3O_2\,(g) \leftrightarrows 6SiO\,(g) + 4N_2\,(g) \quad (6)$$

Therefore, the weight gain during oxidation should result from the formation of SiO_2 and the intermediate layer formed between SiO_2 and Si_3N_4 grains, whose composition features a gradient between SiO_2 and Si_3N_4. This layer, often reported as $Si_xN_yO_z$, functions as diffusion barrier of nitrogen towards the atmosphere, and atmospheric oxygen towards the ceramic bulk.[11,12]

Production process largely defines the porosity of Si_3N_4-ceramics. For instance, reactive sintering results in ceramics with large porosity (>20%), which are obviously not suitable for use in metallurgy industry.[7] Dense Si_3N_4 ceramics are typically produced via liquid phase sintering. There are generally two groups of sintering aids used in Si_3N_4 ceramics. The first group comprises mixtures of oxides which do not form solid solutions with Si_3N_4. The most widely used mixture is Y_2O_3–Al_2O_3, which reacts mainly with SiO_2 formed at the surface of Si_3N_4 grains, resulting in an intergranularly distributed liquid phase, which remains amorphous or partially crystallised after cooling. The second group comprises mixtures of oxides and non-oxides, which form solid solutions with Si_3N_4, such as Y_2O_3–Al_2O_3–AlN and Y_2O_3–AlN. In this case, the partial dissolution of Si_3N_4 results in solid solutions which incorporate a certain amount of additives.[9,13–16]

Yttria (Y_2O_3) essentially determines the formation of Y_2SiO_5, which is precursor of $Y_2Si_2O_7$. The later compound exhibits high resistance towards oxidation since it is the only stable yttrium-containing phase against SiO_2.[14,17,18] The use of Y_2O_3–Al_2O_3 mixtures reduces solidus temperature and lowers viscosity, comparing to the use of pure Y_2O_3, resulting in higher densification but lower thermal stability at elevated temperatures.[16,19]

To the knowledge of the authors, except oxide sintering aids (i.e., Y_2O_3–Al_2O_3),[9,13] there are no reported results on the oxidation behaviour of Si_3N_4 ceramics using nitrides as sintering aids, such as AlN. Moreover, earlier reports on SiAlON ceramics[10,14] have shown that AlN and Si_3N_4 form a solid solution resulting in high densification of ceramics. Therefore, this work investigated the influence of complete and partial substitution of AlN for Al_2O_3 in the sintering aids on the oxidation of Si_3N_4. The interfacial interactions between the Si_3N_4 composition, which exhibited the best behaviour in oxidation conditions, and liquid Al-alloy were experimentally determined at different temperatures and holding times and discussed in the light of thermodynamics.

2. Materials and experimental procedure

Three different types of Si_3N_4 ceramics with compositions $90Si_3N_4$–$5Y_2O_3$–$5Al_2O_3$, $90Si_3N_4$–$5Y_2O_3$–5AlN, and $90Si_3N_4$–$5Y_2O_3$–$2.5Al_2O_3$–2.5AlN (in wt.%) were produced and tested. For simplicity reasons, in this work they will be referred as A, B and C, respectively.

In the previous similar studies, the tested Si_3N_4 samples were of commercial quality.[1–6,8] In this work, they were produced using powders of α-Si_3N_4 (Grade M11, H.C. Starck, Germany, $d = 3.2\,g/cm^3$), α-Al_2O_3 (Grade A16SG, Alcoa Chemicals, USA, $d = 3.98\,g/cm^3$), Y_2O_3 (Grade C-Fine, H.C. Starck, $d = 5.03\,g/cm^3$), and AlN (Grade C, H.C. Starck, $d = 3.26\,g/cm^3$). Suspensions comprising 100 g of appropriate powder mixture and 85 cm^3 of 2-propanol (Riedel de Häen, Aldrich, Germany, $d = 0.87\,g/cm^3$) were prepared. The suspensions were planetary-milled in an Al_2O_3 cube (i.e., milling container) for 4 h, using 300 g of Al_2O_3 balls of different sizes. The weight loss of the Al_2O_3 balls and the cube was always measured. The results indicated that the contamination level introduced in this stage was <0.3%. After drying (40 °C, 72 h), the powders were sieved (80 μm) and calcined at 600 °C for 4 h. Cylindrical pellets (3 g, ∅ 20 mm) were prepared by uniaxial pressing (60 MPa) following by isostatic pressing (200 MPa, 1 min). The green pellets were embedded in a mixture of powders of Si_3N_4 and BN (1:1 weight ratio) inside a graphite crucible and sintered at 1750 °C for 2 h, in nitrogen atmosphere (0.3–0.4 MPa). The weight loss during sintering was measured.

To remove any possible superficial layer formed at the surface of the pellets during sintering, the sintered pellets were rectified and then polished until mirror finishing at both sides. After cleaning in ultrasonic bath with acetone and then with distilled water, the pellets were stored in an oven of 80 °C to avoid water uptake from atmospheric humidity.

The measurements of the density of the pellets (by the Archimedes' method, i.e., immersion in ethylenoglycol,

Riedel de Häen, Aldrich, $d = 1.115\,g/cm^3$) allowed the calculation of the densification of the sintered samples.

Oxidation experiments were carried out in air at 1000 °C until 192 h. The big volume of the furnace chamber ($\sim 2 \times 10^8\,mm^3$) comparing to the size of the pellet ($\sim 3 \times 10^2\,mm^3$) as well as the connection of the chamber with open air ensured abundance of oxygen during oxidation. The weight change of the samples was measured every 24 h of firing (the results are presented with respect to the unit surface area). The crystalline phases were detected by X-ray diffraction (XRD, Rigaku Geigerflex D/Mac, C Series, Cu Kα radiation, Japan). The microstructure of the oxidized surfaces was analysed with scanning electron microscope (SEM, Hitachi S-4100, Japan, equipped with energy dispersive spectroscopy apparatus, EDS).

The experimental procedure for studying the interfacial interactions with molten pure Al (Al99.98) and an Al-foundry alloy (AlSi7Mg, 92.6% Al, 7% Si, 0.4% Mg, in wt.%) was as follows. Discs of Si_3N_4 (either as-sintered or oxidised after sintering at 1000 °C for 192 h) were put together with metal blocks (~25 g) inside high-density Al_2O_3 crucibles (doped with 0.2 wt.% MgO and sintered at 1600 °C for 2 h in air) and heated at 900 and 1100 °C (heating and cooling rates of 10°/min), for 4 or 24 h, under dynamic vacuum (from the total pressure inside the furnace chamber pO_2 was calculated $<2 \times 10^{-3}$ Pa). Cross sections of the obtained ceramic/metal interfaces, polished until 1 μm diamond paste, were analysed by SEM/EDS (EDS at element mapping mode). XRD analysis was employed for detecting reaction products probably formed at the interfaces.

3. Results and discussion

3.1. Sintering ability

The weight loss, which always occurs during sintering of green ceramic bodies, was the lowest one in the ceramics with the lowest content of oxides (i.e., B), specifically 4.48% for A, 1.90% for B, and 4.38% for C. The considerable difference of weight loss between the investigated compositions likely indicates the formation of volatile SiO and AlO, whose formation was favoured under the low O_2 partial pressure conditions of sintering process.[8]

The calculated values of the ratio apparent-density/theoretical-density indicated high densification of all the investigated compositions, specifically 97.27% for A, 98.18% for B, and 97.20% for C (±<0.5%). Experiments with SiAlON ceramics have shown that Y_2O_3 and the nitrides Si_3N_4 and AlN can form solid solutions resulting in complete dense materials,[10,14] which is in accordance with the highest densification of composition B.

According to earlier studies, the stages of sintering should be as follows: (a) reaction of SiO_2 film, already formed at the surface of Si_3N_4 particles, with sintering additives; (b) formation of a liquid phase; (c) dissolution and diffusion of α-Si_3N_4 in the liquid; and (d) precipitation of β-Si_3N_4.[14,20]

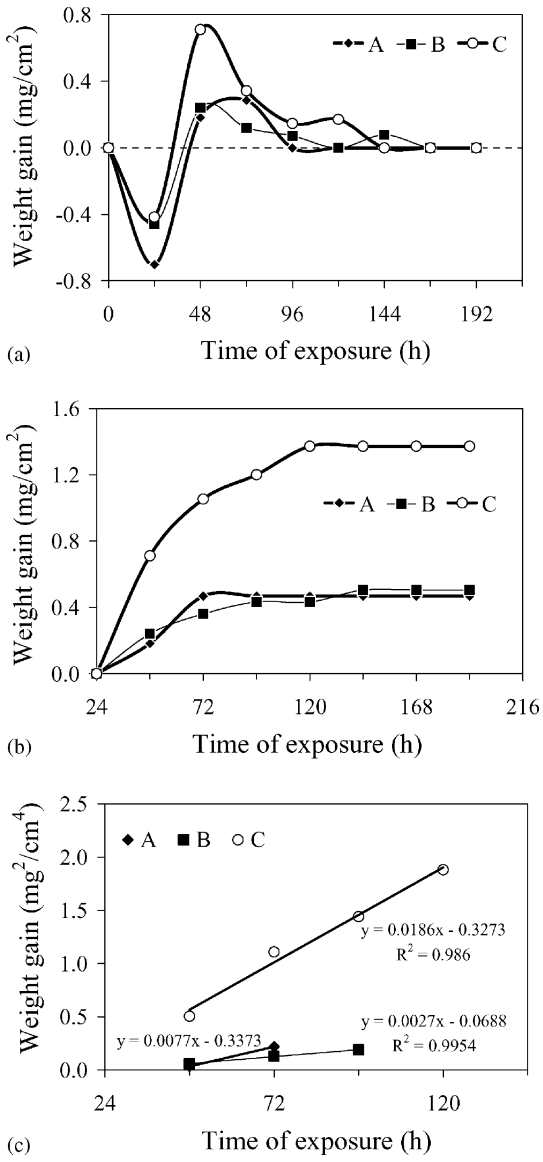

Fig. 1. Weight change of the investigated compositions A, B and C over exposure time in air at 1000 °C: (a) differential plot; (b) cumulative plot considering as initial weight that one measured after 24 h of heating; (c) plot of weight gain from the beginning of the experiments according to the parabolic law of Eq. (1), where the points of weight loss (i.e., at 24 h) as well as the points where there was no actual increase of the weight of the samples (i.e., at the plateu of panel b) have not been considered.

3.2. Oxidation

Fig. 1a plots the weight gain over exposure time to air at 1000 °C. Weight loss was observed only after 24 h (but it was more pronounced in A). Similar weight loss has been reported in the case of Si_3N_4–SiC ceramics after similar heat treatment (1000 °C until 138 h), attributed to the Eqs. (5) and (6).[8] In the present study, the large volume of the furnace chamber and the connection of the chamber with open

air should favour these chemical reactions. Neglecting this effect, Fig. 1b and c shows that the weight gain followed parabolic evolution (Eq. (1)).

The curves of Fig. 1b reach a plateau after 72 h of heating for A, 96 h for B, and 120 h for C. The plateau must indicate the complete formation of a superficial oxide layer which can provide the highest protection against oxidation. The richest composition in oxides (i.e., A) reached faster this regime than the others. The complete formation of this protective layer might be assigned to the maximum devitrification state of materials since crystallized materials generally feature higher chemical stability than the corresponding glassy ones.

Fig. 2 allows the comparison of the influence of oxides and nitrides sintering additives on the microstructure (shown at fracture surfaces and top views) of Si_3N_4-ceramics under oxidation conditions. A thin layer (<2 μm) was formed on the surface of the oxidized samples of composition A, while edges of crystals, probably of Si_3N_4, can be the observed under this layer (Fig. 2a). The microstructure of the surface was slightly porous (Fig. 2b). It is difficult to observe any oxide layer at the surface of samples of composition B, whose microstructure was fine (Fig. 2c and d). In composition C, the Si_3N_4 crystals were covered with a thick oxide layer (∼10–12 Nm) (Fig. 2e and f).

Fig. 2 reveals that prolonged oxidation caused increasing surface roughness. Nevertheless, the effect of increasing exposure surface area over oxidation time was impossible to be taken into account in the plots of Fig. 1. Thus, the plots of Fig. 1 were calculated with respect to the initial polished flat area of the pellets.

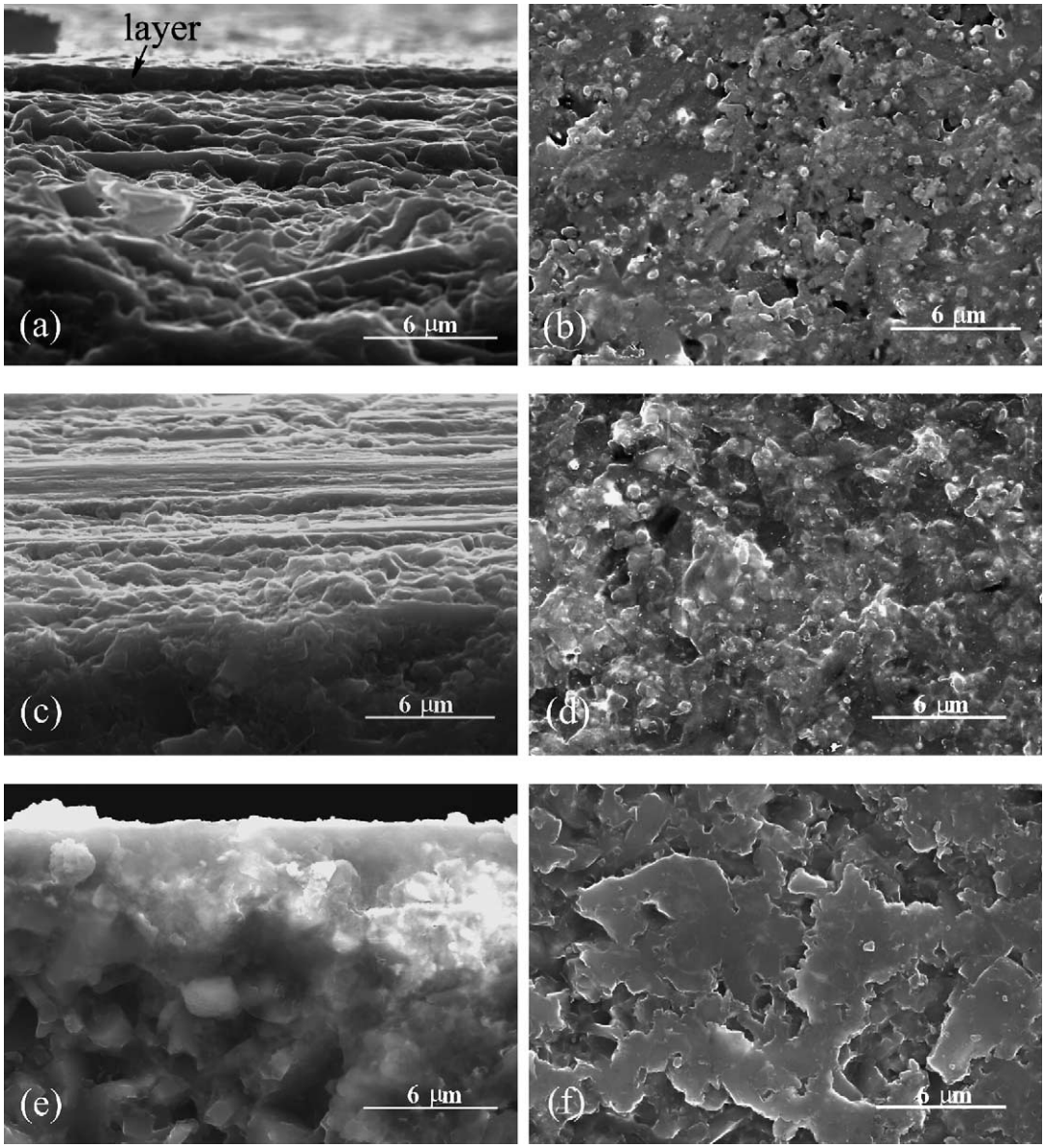

Fig. 2. Microstructure observed at fracture surfaces and top views of the surfaces of the investigated Si_3N_4 compositions A (a and b), B (c and d), and C (e and f), after oxidation at 1000 °C for 192 h.

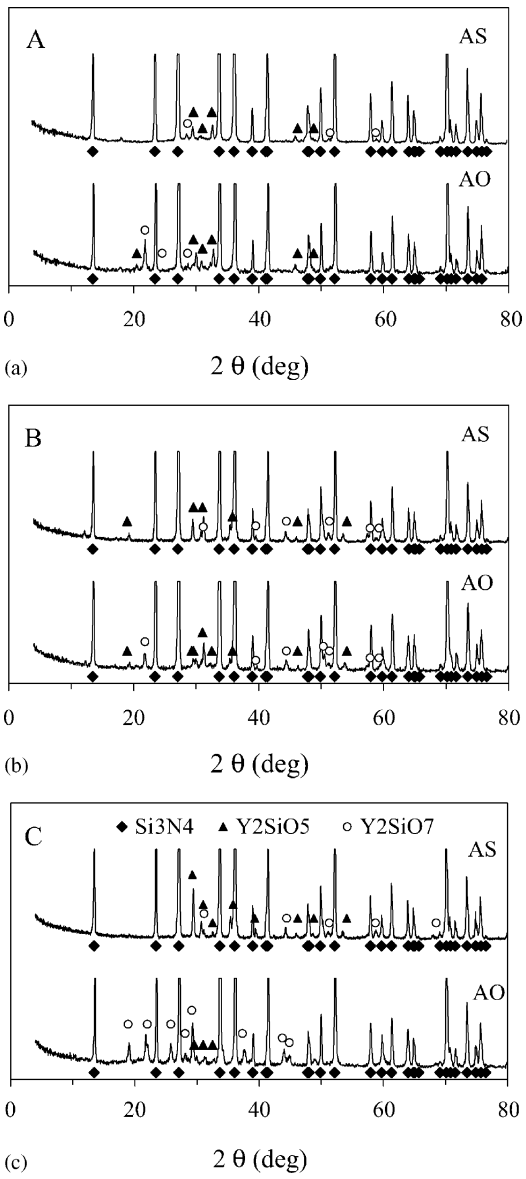

Fig. 3. XRD spectra of the investigated compositions A (a), B (b) and C (c), after sintering (AS) and after oxidation (AO) in air at 1000 °C for 192 h. JCPDS cards: β-Si_3N_4: 33-1160; Y_2SiO_5: 41-0004; $Y_2Si_2O_7$: 82-0732. In the spectrum of composition C after oxidation (c: AO) the phase of $Y_2Si_2O_7$ was identified using the JCPDS card 48-1623.

XRD analysis (Fig. 3) showed that together with β-Si_3N_4, Y_2SiO_5 predominantly formed during sintering (presence of traces of $Y_2Si_2O_7$ might be also suggested), while oxidation mainly resulted in formation of $Y_2Si_2O_7$. These results support the aforementioned stages of sintering and agree fairly well with earlier studies with Si_3N_4-ceramics doped with oxide additives.[9,13] The effect of oxidation was more pronounced in composition C (Fig. 3c), which agrees fairly well with Fig. 2e and f. It is worthy nothing that the identification of the X-ray patterns which correspond to $Y_2Si_2O_7$ revealed that at low concentration regime, $Y_2Si_2O_7$ crystallizes in orthorhombic system (plots of Fig. 3a–c: AS; JCPDS card 82-0732) while in a regime of abundance the strong peaks correspond to monoclinic lattice (plot of Fig. 3c: AO; JCPDS card 48-1623).

The aforementioned results indicate that the compositions A and B should anticipate reliable performance in relatively high temperature applications since they featured dense microstructures and favoured the formation of superficial thin films, which resist to further oxidation, in comparison with composition C. Fig. 1b indicates that composition A reaches faster the equilibrium regime with regard to the formation of the superficial oxide layer. Therefore, the experiments for determining the interfacial interactions with molten aluminium alloys were carried out with composition A.

3.3. Ceramic/metal interfaces

3.3.1. Microstructure

The interfaces between Si_3N_4 ceramics of composition A ($90Si_3N_4$–$5Y_2O_3$–$5Al_2O_3$) and liquid Al-containing phases at several temperatures and times, are characteristically depicted in Figs. 4–6, in the form of the distribution of Al and Si across the interface (element mapping). In general, the investigated ceramics exhibited high chemical stability towards liquid Al-alloy since there was no evidence of intensive chemical reaction, such as irregularities along ceramic/metal interfaces or formation of separated reaction zones with different composition than those of the contacting phases, even over prolonged experiments (24 h). X-ray diffraction analysis (not shown) did not identify newly formed phases. The interfaces were continuous and featured no gaps or cracks, as characteristically shown in Fig. 4a. After the experiments, several times the Si_3N_4 pellets were found not entirely immersed in the Al-alloy. In these cases, the contact angles visually observed between ceramic and metal were $<90°$. Beyond these general characteristics, careful observation can provide more detailed information for each experimental condition, outlined as follows.

In the samples heated at 900 °C for 4 h, solidified Si-rich clusters were homogeneously distributed in the metal phase (Fig. 4b–e). AlSi7Mg alloys typically feature similar structures of Si-rich phase dispersed in the aluminium matrix.[21] Pre-oxidation of ceramics had no perceptible effect on the interface at this temperature (Fig. 4f and g). The Si-rich irregularities observed at the metal side of interface (shown by the arrow in Fig. 4f) should be attributed to the superficial layer formed during oxidation, resulting in increasing surface roughness (Fig. 2a and b).[1]

Heat treatment at 1100 °C for 4 h (Fig. 5a and b) or 24 h (Fig. 5c and d) had no effect on the high inertness of ceramics. In prolonged experiments (24 h), a tiny shadowed zone (~5 μm) seemingly exists at the metal side along the interface (Fig. 5c) and might indicate the formation of a diffusion zone between the contacting phases. Pre-oxidation of ceramics has seemingly more sound effect at the interfaces tested at this temperature (Fig. 6). Islets enriched in Si were seemingly migrated towards the metal, regardless the nature

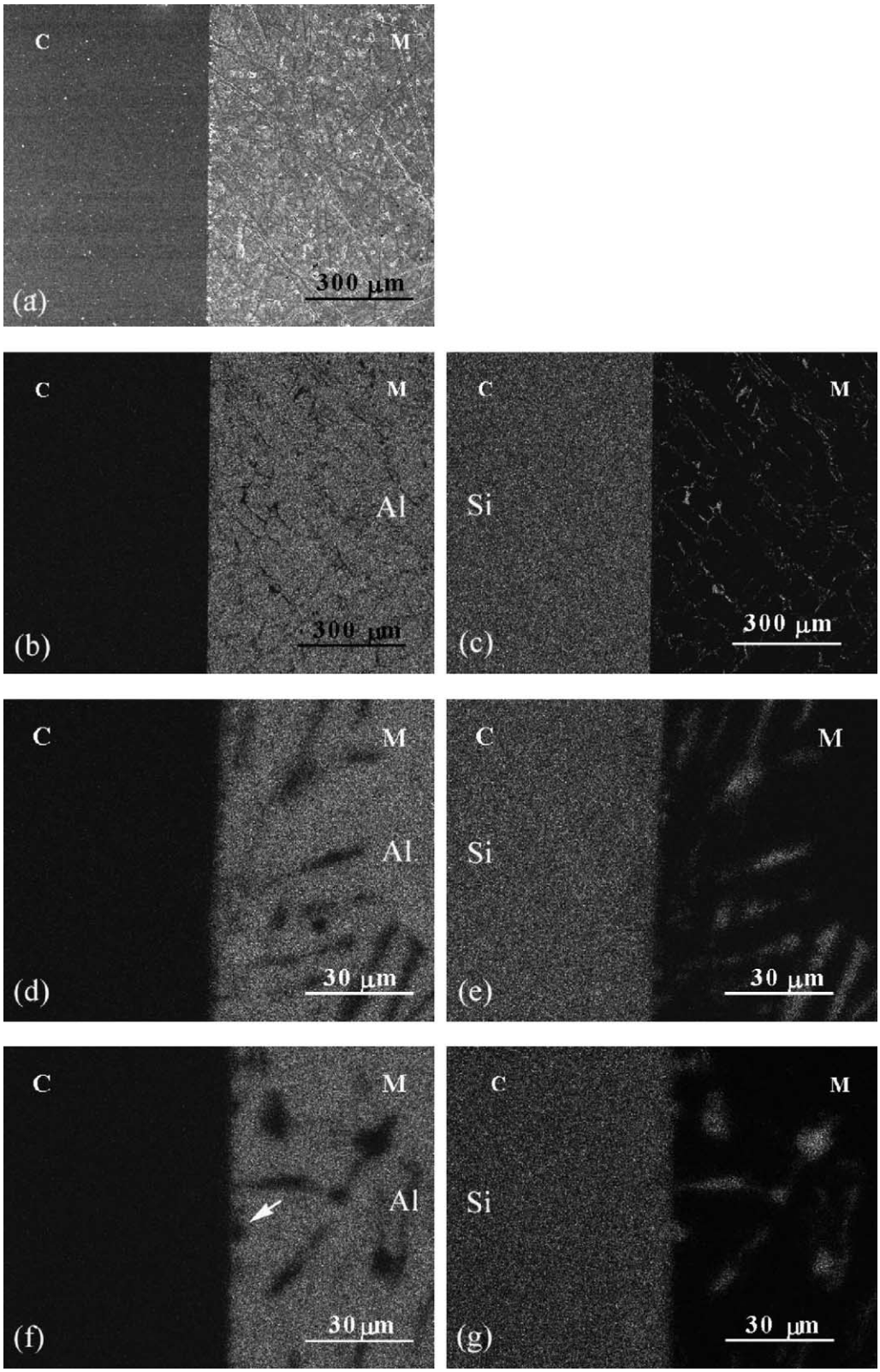

Fig. 4. Cross section at interfaces between composition A ($90Si_3N_4$–$5Y_2O_3$–$5Al_2O_3$) and AlSi7Mg after heat treatment at 900 °C for 4 h: mirostucture (a) and element mapping scan (Al and Si) at low (b and c) and high magnification (d and e); element mapping at interfaces where the Si_3N_4 ceramics were preoxidized at 1000 °C for 192 h. (In the element maps, the identified element appears with light colour; M: metal; C: ceramic).

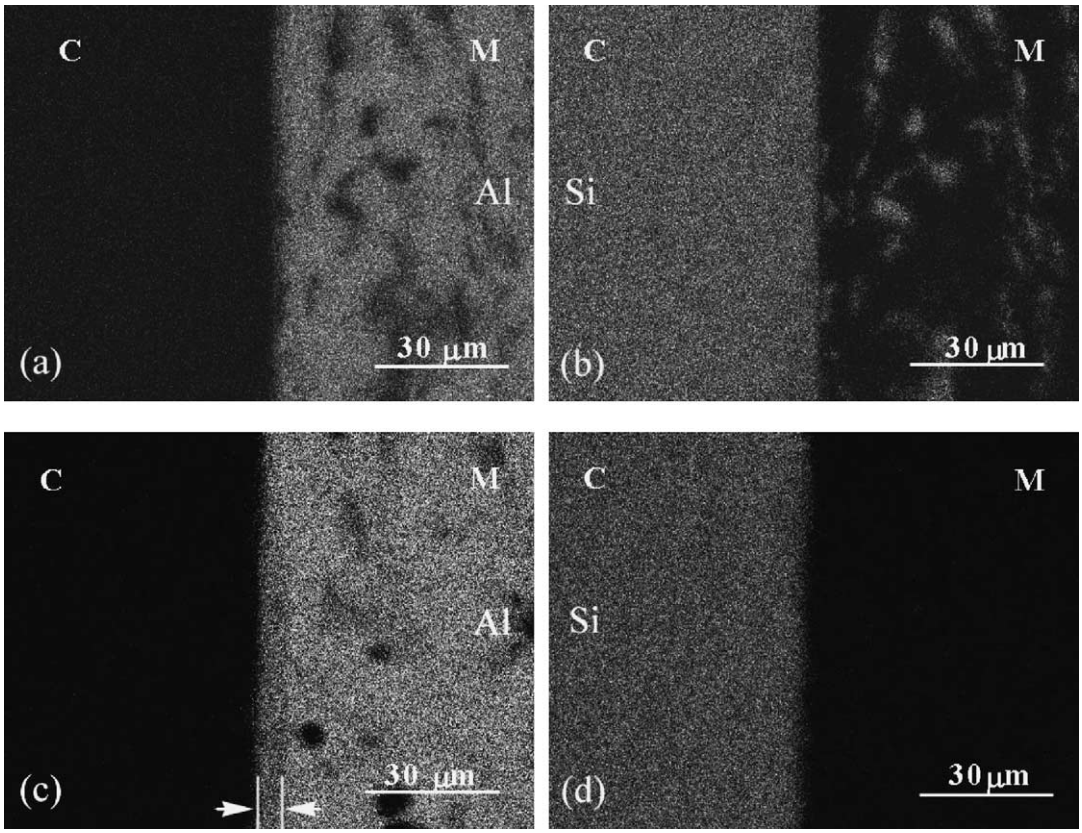

Fig. 5. Distribution of Al and Si at interfaces between composition A ($90Si_3N_4$–$5Y_2O_3$–$5Al_2O_3$) and AlSi7Mg after heat treatment at 1100 °C for 4 h (a and b) and 24 h (c and d). (The identified element appears with light colour; M: metal; C: ceramic).

of liquid phase (i.e., Al-alloy, Fig. 6a and b, or pure Al, Fig. 6c and d).

3.3.2. Interfacial interactions and adhesion

The prolonged experiments (until 24 h) at such high temperatures imply that there should be no factors which might delay the kinetics of the investigated ceramic/metal reactions and whose action would be revealed over longer (i.e., >24 h) experiments. In the light of this assumption, the experimental results demonstrated that there is no intensive chemical reaction between the investigated ceramics and liquid Al-alloys. Nevertheless, the reaction between Si_3N_4 and Al described by the following chemical equation

$$Si_3N_4\,(s) + 4Al\,(l) \rightarrow 4AlN\,(s) + 3Si\,(l) \quad (7)$$

is thermodynamically favourable at 1000 °C since $\Delta G = -99.1$ kJ/mol of Al (1000 °C is the average temperature of the experiments and can be considered as a high temperature in Al-foundry industry).[22] The earlier sections of this article also impose the existence of SiO_2. Nevertheless, its presence leads the ceramic to a vulnerable regime ($\Delta G_{(8)} < \Delta G_{(7)}$):[22]

$$3SiO_2\,(s) + 4Al\,(l) \rightarrow 2Al_2O_3\,(s) + 3Si\,(l)$$
$$\Delta G_{1000\,^\circ C} = -123.2\,\text{kJ/mol Al} \quad (8)$$

However, it is well known that yttria exhibits remarkable stability against liquid aluminium.[1,7] The X-ray spectra of Fig. 3a showed that the investigated ceramics also contained the yttrium-containing phases Y_2SiO_5 and traces of $Y_2Si_2O_7$. The complete dissociation of these ternary yttrium silicates from Al to Al_2O_3 possesses positive of slightly negative chemical potential, respectively:[22]

$$3Y_2SiO_5\,(s) + 10Al\,(l) \rightarrow 5Al_2O_3\,(s) + 3Si\,(l) + 6Y\,(l)$$
$$\Delta G_{1000\,^\circ C} = -32.5\,\text{kJ/mol Al} \quad (9)$$

$$3Y_2Si_2O_7\,(s) + 14Al\,(l) \rightarrow 7Al_2O_3\,(s) + 6Si\,(l) + 6Y\,(l)$$
$$\Delta G_{1000\,^\circ C} = -12.0\,\text{kJ/mol Al} \quad (10)$$

Nevertheless, from the phase diagrams between Y_2O_3, SiO_2 and Al_2O_3, except Y_2SiO_5 and $Y_2Si_2O_7$, $Y_4Si_3O_{12}$, $Y_4Al_2O_9$, $YAlO_3$ and $Y_3Al_5O_{12}$ are also predicted. Although neither SEM nor XRD detected newly formed phases at the interfaces after the experiments, calculations of ΔG values indicate that the substitution of Al for Si in the yttrium silicates to form ternary yttrium aluminates is thermodynamically highly favourable, as shown in the following equation, just to refer one:

$$3Y_2Si_2O_7 + 8Al \rightarrow 5Y_3Al_5O_{12} + 6Si + 3YAlO_3$$
$$\Delta G_{1000\,^\circ C} = -119.86\,\text{kJ/mol Al} \quad (11)$$

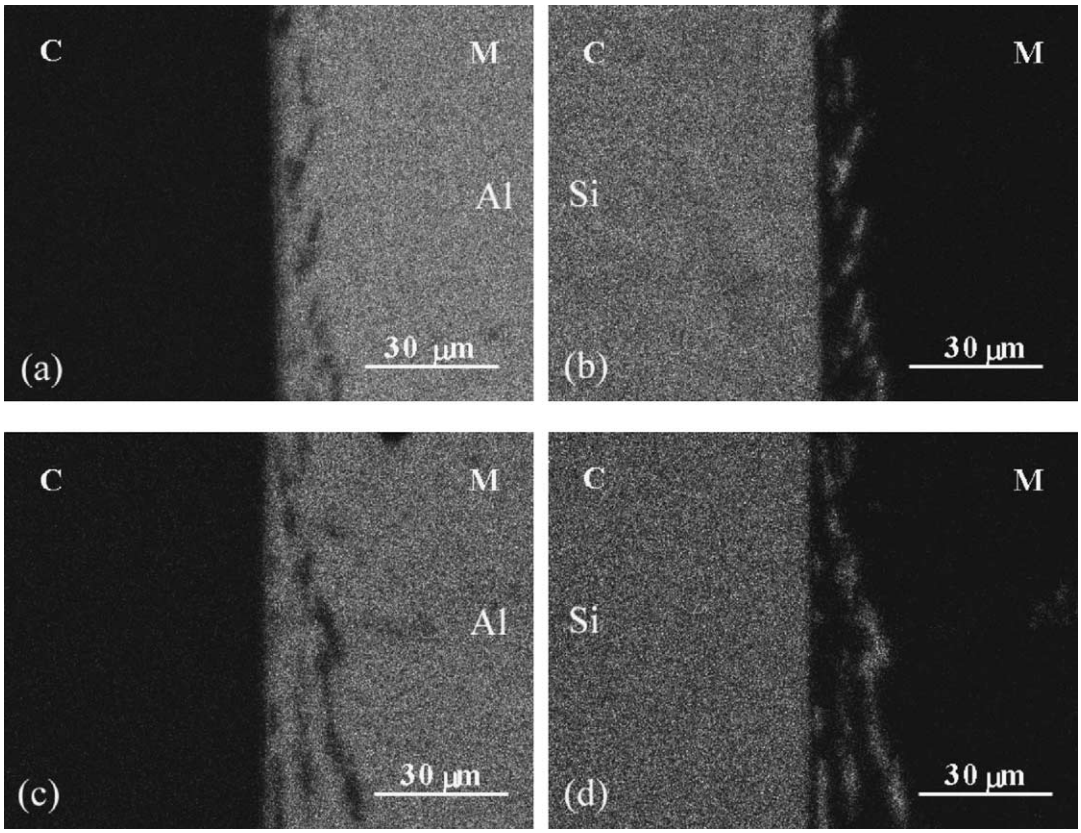

Fig. 6. Distribution of Al and Si at interfaces between preoxidized (1000 °C, 192 h) Si_3N_4 ceramics of composition A ($90Si_3N_4$–$5Y_2O_3$–$5Al_2O_3$) and AlSi7Mg (a and b) and Al99.98 (c and d) after heat treatment at 1100 °C for 4 h. (The identified element appears with light colour; M: metal; C: ceramic).

Therefore, the formation of yttrium aluminates, whose formation is thermodynamically anticipated, must be assumed. Their concentration was probably below the sensitivity of the employed apparatus under the particular experiment procedure. Their low concentration can be attributed to the overall low concentration of the yttrium silicates in the ceramic materials as well as the limited contacting solid/liquid area (i.e., no infiltration). In the light of the highly negative ΔG-values of the Eqs. (7) and (8), these phases of yttrium aluminates should act as diffusion barriers at the solid/liquid interface which moderate or suppress the possibility of occurrence of the reactions of the Eqs. (7) and (8).

Consequently, mild diffusion should govern the ceramic/liquid metal interfacial interactions. The possible diffusion zone observed in the shadowed ribbon in Fig. 5c is very thin, with respect to the prolonged heating (24 h). Thus, the diffusion kinetics should be very slow. However, the present experimental results cannot assure that this possible zone was formed when the Al-alloy was still in molten state or during cooling.

In the case of pre-oxidized samples, the migration of Si-rich islets towards the metal bulk (Fig. 6) may resemble results obtained in solid state diffusion, where chemically stable markers can be used to determine experimentally the Kirkendall plane in a diffusion couple.[23] If similar mechanism can generally approach the investigated systems, which certainly differ from solid state diffusion couples since one phase was in liquid state, then there should be a difference of the diffusion coefficients at the interface (for instance, those of Si to Al-melt and Al to Si_3N_4). This difference should have caused the migration of either the phase formed at the surface of the ceramic after the pre-oxidation or a product of this phase after a reaction with liquid Al, or a combination of both phenomena.

The microstructure of the fracture surface shown in Fig. 2a indicates that the adhesion between the superficial layer formed after oxidation and the parent ceramic is lower than the cohesion of either the layer or the bulk ceramic. However, the SEM micrographs of Fig. 6 do not indicate presence of well separated islets of different phases in the metal phase. Therefore, the observed islets of Fig. 6 are probably Si-rich clusters (similar to those shown in Figs. 4 and 5).[21] Eqs. (10) and (11) show two possibilities of formation of Si due to reaction of $Y_2Si_2O_7$, which is the main product of oxidation, with Al. At lower temperatures (900 °C, Fig. 4f and g), the difference of diffusion coefficients is probably small and cannot cause detectable migration of such phases.

With regard to interfacial adhesion, the interfaces were continuous with no gaps or cracks. In the literature, the good wetting between Al and Si_3N_4-based ceramics at temperatures higher than 827 °C has been attributed to the reac-

tion which results in formation of AlN.[7] In this study, the presence of Si in the alloy likely improved liquid metal's fluidity[21] and bettered wettability, resulted in the strong and continuous interface. Several authors have reported that the presence of sintering additives and/or the formation of a superficial oxide layer favours Si_3N_4/liquid metal adhesion at elevated temperatures and prolonged contact.[1–6] The same effect has been observed in SiC-based ceramics.[8,24]

Beyond refractory properties of ceramics, which is a key issue in Al-foundry industry and motivated the present study as mentioned in the Introduction, this study features interesting results for producing Si_3N_4–metal composites. Strong adhesion and continuous interfaces were achieved with no formation of new phases, whose probable brittleness and mismatch of thermal expansion coefficients with the parent materials would result in a failure of interface.[1–5,25–29]

In general, this work agrees fairly well with earlier studies,[1–8,24–27] which have reported that decomposition of Si_3N_4-based ceramics by liquid aluminium and its alloys, even under low oxygen partial pressure and high temperature conditions, is very difficult. The presence of alloying elements often influences ceramic/metal interactions.[4,30] However, there was no evidence of such effect in this study (Fig. 6).

4. Conclusions

Sintering aids containing Y_2O_3 influence the microstructure and the crystalline-state of Si_3N_4-ceramics produced via pressureless liquid state sintering, and determine their response towards oxidation. Sintering predominantly results in formation of Y_2SiO_5 as secondary phase after Si_3N_4, while $Y_2Si_2O_7$ mainly forms after oxidation. The superficial layers, formed after oxidation, are thinner and formed faster in the compositions $90Si_3N_4$–$5Y_2O_3$–$5Al_2O_3$ and $90Si_3N_4$–$5Y_2O_3$–5AlN than in the composition $90Si_3N_4$–$5Y_2O_3$–$2.5Al_2O_3$–2.5AlN.

Mild diffusion seemingly governs the interfacial interactions between $90Si_3N_4$–$5Y_2O_3$–$5Al_2O_3$ ceramics and liquid AlSiMg-alloy. Compounds, whose formation results from the yttria-containing sintering aids, such as yttrium aluminates, should act as diffusion barriers at the ceramic/liquid metal interface. The interfacial adhesion was generally good, since the ceramic/metal interface was continuous, with no gaps or cracks. These results are interesting for applications in both Al-foundry industry and production of Si_3N_4–Al composites.

Acknowledgements

The financial support of the Portuguese Foundation of Science and Technology (S.A.) is gratefully acknowledged.

References

1. Morita, M., Suganuma, K. and Okamoto, T., Effect of pre-heat-treatment on silicon nitride joining with aluminium braze. *J. Mater. Sci. Lett.* 1987, **6**, 474–476.
2. Ning, X. S., Suganuma, K., Okamoto, T., Miyamoto, Y. and Koreeda, A., Effect of oxide additive in silicon nitride on interfacial structure and strength of silicon nitride joints brazed with aluminium. *J. Mater. Sci.* 1989, **24**, 2865–2870.
3. Ning, X. S., Suganuma, K., Okamoto, T., Koreeda, A. and Miyamoto, Y., Interfacial strength and chemistry of additive-free silicon nitride ceramics brazed with aluminium. *J. Mater. Sci.* 1989, **24**, 2879–2883.
4. Ning, X. S., Okamoto, T., Suganuma, K., Miyamoto, Y., Koreeda, A. and Goda, S., Bond strength and interfacial structure of silicon nitride joints brazed with aluminium-silicon and aluminium-magnesium alloys. *J. Mater. Sci.* 1991, **26**, 2050–2056.
5. Ning, X. S., Okamoto, T., Suganuma, K., Miyamoto, Y. and Koreeda, A., Reaction chemistry at joined interfaces between silicon nitride and aluminium. *J. Mater. Sci.* 1991, **26**, 4142–4149.
6. Suganuma, K., Okamoto, T., Koizumi, M. and Shimada, M., Joining of silicon nitride to silicon nitride and to Invar alloy using an aluminium interlayer. *J. Mater. Sci.* 1987, **22**, 1359–1364.
7. Schwabe, U., Wolff, L. R., van Loo, F. J. J. and Ziegler, G., Corrosion of technical ceramics by molten aluminium. *J. Eur. Ceram. Soc.* 1992, **9**, 407–415.
8. Johnston, M. W. and Little, J. A., Degradation of oxidized SiC–Si_3N_4 in molten aluminium. *J. Mater. Sci.* 1990, **25**, 5284–5290.
9. Cinibulk, M. K. and Thomas, G., Oxidation behaviour of rare-earth disilicate-silicon nitride ceramics. *J. Am. Ceram. Soc.* 1992, **75**, 2044–2049.
10. Nickel, K. G., Corrosion of non-oxide ceramics. *Ceram. Int.* 1997, **23**, 127–133.
11. Ogbuji, L. U. J. T., The SiO_2–Si_3N_4 interface. Part II: O_2 permeation and oxidation reaction. *J. Am. Ceram. Soc.* 1995, **78**, 1279–1284.
12. Backhaus-Ricoult, M. and Gogotsi, Y. G., Identification of oxidation mechanisms in silicon nitride ceramics by transmission electron microscopy studies of oxide scales. *J. Mater. Res.* 1995, **10**, 2306–2321.
13. Singhal, S. C., Thermodynamics and kinetics of oxidation of hot-pressed silicon nitride. *J. Mater. Sci.* 1976, **11**, 500–509.
14. Lange, F. F., Fabrication and properties of dense polyphase silicon nitride. *Ceram. Bull.* 1983, **62**, 1369–1374.
15. O'Meara, C. and Sjoeberg, J., Transmission electron microscopy investigation of the oxidation of hot isostatically pressed silicon nitride with and without sintering aids. *J. Am. Ceram. Soc.* 1997, **80**, 1491–1500.
16. Ziegler, G., Heinrich, J. and Woetting, G., Review: relationships between processing, microstructure and properties of dense and reaction-bonded silicon nitride. *J. Mater. Sci.* 1987, **22**, 3041–3086.
17. Cinibulk, M. K. and Kleebe, H.-J., Effects of oxidation on intergranular phases in silicon nitride ceramics. *J. Mater. Sci.* 1993, **28**, 5775–5782.
18. Kolitsch, U., Seifert, H. J., Ludwig, T. and Aldinger, F., Phase equilibria and crystal chemistry in the Y_2O_3–Al_2O_3–SiO_2 system. *J. Mater. Res.* 1999, **14**, 447–455.
19. Lewis, M. H. and Barnard, P., Oxidation mechanisms in Si-Al-O-N. *J. Mater. Sci.* 1980, **15**, 443–448.
20. Ordoñez, S., Iturriza, I. and Castro, F., The influence of amount and type of additives on α-β Si_3N_4 transformation. *J. Mater. Sci.* 1999, **34**, 147–153.
21. Davis J. R., *Aluminum and Aluminum Alloys*. ASM Speciality Book, Materials Park, OH, 1996.
22. JANAF Thermochemical Tables, *J. Phys. Chem. Ref. Data* 1985, **14**, 165.
23. van Loo, F. J. J., Multiphase diffusion in binary and ternary solid-state systems. *Prog. Solid State Chem.* 1990, **20**, 47–99.

24. Laurent, V., Chatain, D. and Eustathopoulos, N., Wettability of SiC by aluminium and Al-Si alloys. *J. Mater. Sci.* 1987, **22**, 244–250.
25. Mouradoff, L., Lachau-Durand, A., Desmaison, J., Labbe, J. C., Grisot, O. and Rezakhanlou, R., Study of the interaction between liquid aluminium and silicon nitride. *J. Eur. Ceram. Soc.* 1994, **13**, 323–328.
26. Nicholas, M. G., Mortimer, D. A., Jones, L. M. and Crispin, R. M., Some observations on the wetting and bonding of nitride ceramics. *J. Mater. Sci.* 1990, **25**, 2679–2689.
27. Tomsia A. P., Saiz E., Dalgleish B. J. and Cannon R. M., Wetting and strength issues in ceramic/metal bonding. In *Challenging to Future Advanced Materials Aiming for Intelligence and Harmonization. Proceedings of the 4th Japan International SAMPE Symposium*, September 25–28, 1995, pp. 347–356.
28. Oliveira, M. and Ferreira, J. M. F., Structural and mechanical characterisation of MgO-, CaO- and BaO-doped aluminosilicate ceramics. *Mater. Sci. Eng.* 2003, **A344**, 35–44.
29. Mouradoff, L., Tristant, P., Desmaison, J., Labbe, J. C., Desmaison-Brut, M. and Rezakhanlou, R., Interaction between liquid aluminium and non-oxide ceramics. *Key Eng. Mater.* 1996, **113**, 177–186.
30. Naka, M., Kubo, M., Okamoto, T., Koizumi, M. and Shimada, M., Joining of silicon nitride with Al-Cu interlayers. *J. Mater. Sci.* 1987, **22**, 4417–4421.